

Antioxidant and Cytoprotective Effects of New Diarylheptanoids from *Rhynchanthus beesianus*

Pei-Feng Zhu,[#] Gui-Guang Cheng,[#] Lan-Qin Zhao, Afsar Khan, Xing-Wei Yang, Bu-Yun Zhang, Meng-Cheng Li, Ya-Ping Liu,^{*} and Xiao-Dong Luo^{*}

 Cite This: *J. Agric. Food Chem.* 2021, 69, 6229–6239

 Read Online

ACCESS |

 Metrics & More

 Article Recommendations

 Supporting Information

ABSTRACT: *Rhynchanthus beesianus* (Zingiberaceae) has been an important food spice and vegetable in southern China. Fifteen phenolic compounds (1–15) including three new diarylheptanoids, rhynchanines A–C (1–3) and one new phenylpropanoid, 4-O-methylstroside B (9), were isolated from *R. beesianus* rhizomes. The structures of new compounds were elucidated by comprehensive analyses through NMR, HRMS technique, acid hydrolysis, and Mosher's reaction. Among them, compound 5 is the first isolated natural product and its NMR data are reported. Most of the isolated compounds, especially 3–6 and 8, showed significant antioxidant activities on DPPH, ABTS⁺ radical scavenging, and FRAP assays. Furthermore, the antioxidant phenolic compounds were evaluated for their cytoprotective capacity against H₂O₂-induced oxidative stress in HepG-2 cells. Compounds 3 and 5 could significantly inhibit reactive oxygen species production, and compounds 3, 5, and 6 could remarkably prevent the cell apoptosis. Then, the *R. beesianus* rhizome, which contained phenolic compounds, might serve as a functional food for potential application on preventing oxidative stress-connected diseases.

KEYWORDS: *Rhynchanthus beesianus*, diarylheptanoid, antioxidant activity, intracellular reactive oxygen species, cell apoptosis

INTRODUCTION

Reactive oxygen species (ROS), the major etiological factor of oxidative stress, could cause cell damage and apoptosis when these are excessively produced.^{1,2} The excessive production of ROS accelerates aging and increases the risk of diseases, for example, Alzheimer's disease, diabetes, atherosclerosis, Parkinson's disease, and cancer. Fortunately, antioxidants could efficiently retard the process of these disorders.^{3,4} A number of antioxidants, including phenols, flavonoids, polysaccharides, and tannins, have been proved to reduce oxidative damage through scavenging radicals, metal chelation, and promotion of the expression of antioxidant and phase II metabolic enzymes.⁵ Studies have shown that the intake of natural antioxidants has good protective effects on oxidative stress-induced degenerative diseases.^{2,6} As a vital class of natural antioxidants, phenolics have attracted particular attention for their high contents in daily diets.^{7–9}

Diarylheptanoids, composed of two aromatic rings linked by a heptane skeleton, are an important group of natural polyphenols with various bioactives.¹⁰ The diarylheptanoids are commonly present in linear and cyclic forms, and the latter usually contain a six-membered tetrahydropyran moiety.¹¹ Previous pharmacological investigations demonstrated that the diarylheptanoids have remarkable antioxidant, antitumor, antidepressant, antitubercular, neuroprotective, and estrogenic effects.^{10–15} In recent decade, various diarylheptanoids have been isolated from edible plants of *Curcuma*, *Alpinia*, *Zingiber* (Zingiberaceae), *Myrica* (Myricaceae), *Corylus* (Betulaceae), *Garuga* (Burseraceae), and *Juglans* (Juglandaceae) genera.^{11,16,17}

The genus *Rhynchanthus* Hook.f. (Zingiberaceae) is a small genus with about six species.¹⁸ *Rhynchanthus beesianus* is the only species of this genus that is distributed in southern China.¹⁹ It is an edible, ornamental, and medicinal plant with tuberous rhizomes, having unique aroma and taste compared with other edible gingers. Besides being an important blending agent in kitchen, the tender leaves and tuberous rhizomes of *R. beesianus* are widely and traditionally consumed as vegetables and edible spices.^{20,21} Additionally, *R. beesianus* rhizomes have been traditionally used as folk medicine for regulating various gastrointestinal disorders including abdominal discomfort, dyspepsia, belching, and bloating.^{19,20} Previous studies reported that the essential oil from *R. beesianus* rhizomes exhibited anti-inflammatory and antibacterial activities.^{19,20} However, until now, there is no report on the nonvolatile components of *R. beesianus* rhizome and their antioxidant activity. Therefore, the aim of this research was to illustrate the chemical components from *R. beesianus* rhizomes and evaluate their antioxidant and cytoprotective activities.

Phytochemical investigation on *R. beesianus* rhizomes resulted in 15 polyphenols, including three new diarylheptanoids rhynchanines A–C (1–3) and one new phenylpropanoid, 4-O-methylstroside B (9). Compound 5 had been reported only by LC–MS identification from *Curcuma longa*;²²

Received: February 13, 2021

Revised: April 30, 2021

Accepted: May 3, 2021

Published: May 24, 2021



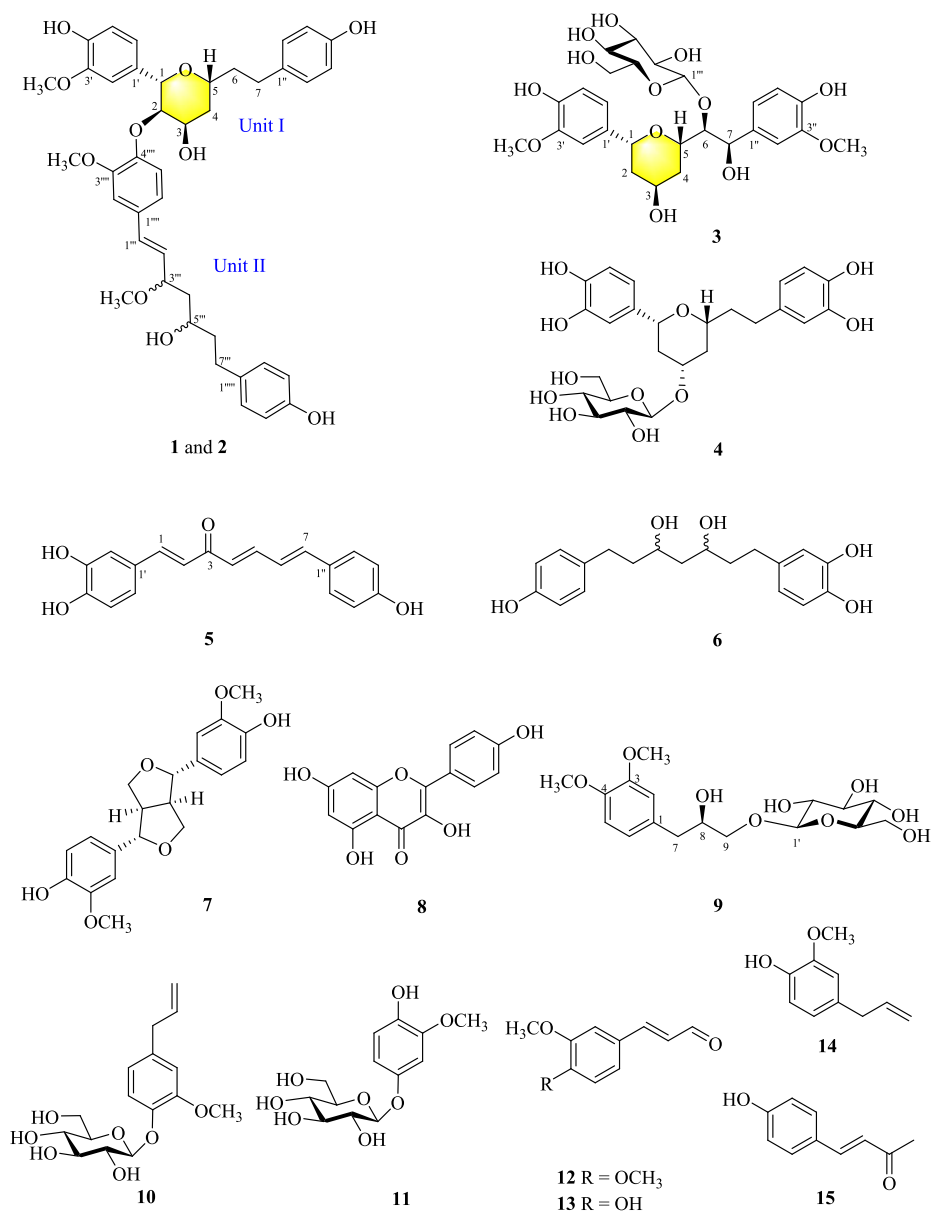


Figure 1. Compounds 1–15 from *R. beesianus*.

herein, **5** is isolated as a pure monomer and its NMR data are assigned for the first time. The antioxidant capacity of compounds 1–15 was assessed by DPPH, ABTS⁺, and FRAP assays. Additionally, the antioxidant phytochemicals were tested for their protective effect on oxidative stress in H₂O₂-induced human liver HepG-2 cells. The cytoprotective capacity was assessed for regulating the intracellular ROS production and cell apoptosis by flow cytometry. Compounds **3** and **5** significantly inhibited ROS production, while compounds **3**, **5**, and **6** remarkably prevented the cell apoptosis.

MATERIALS AND METHODS

General Experimental Procedures and Reagents. Optical rotations were measured on a JASCO P-1020 polarimeter. The UV spectra were recorded on a Shimadzu UV-2401PC spectrometer. The IR spectra were measured on a Bruker FT-IR Tensor-27 infrared spectrophotometer with KBr disk. The NMR spectra were obtained on Bruker DRX-400, DRX-500, and DRX-600 spectrometers. Chemical shifts (δ) were expressed in ppm with reference to the

solvent signals. MS data were measured on Waters Xevo TQS or Waters AutoSpec Premier P776 mass spectrometers. Semipreparative HPLC was performed on a Waters 600 with a COSMOSIL C₁₈ (10 × 250 mm, NacalaiTesque Corporation, Japan) column and analytical HPLC was performed on a Shimadzu SIL-20A Series HPLC system equipped with a reverse-phase COSMOSIL C₁₈ column (4.6 mm × 250 mm, 5 μ m, NacalaiTesque Corporation, Japan). Silica gel (200–300 mesh, Qingdao Marine Chemical Co., Ltd., China), MCI-gel (75–150 μ m, Mitsubishi Chemical Corporation, Japan), YMC-gel (50 μ m, YMC Co., Ltd., Japan), and RP-C₁₈ column (40–63 μ m, Merck Drugs & Biotechnology, Germany) were used for column chromatography. The PMP (Chengdu Aikeda Chemical Reagent Co., Ltd., China), 2,2-diphenyl-1-picrylhydrazyl (DPPH) radical, methylthiazol-2-yl-2,5-diphenyltetrazoliumbromide (MTT), 2,2'-azino-bis(3-ethyl-benzothiazoline-6-sulfonic acid) (ABTS), 2',7'-dichlorofluoresceindiacetate (DCFH-DA), and 1,3,5-tri(2-pyridyl)-2,4,6-triazine (TPTZ) were purchased from Sigma-Aldrich (Shanghai, China). A flow cytometer (Guava easyCyte 6-2L, Millipore, Billerica, USA) and Annexin V-FITC/PI apoptosis kit were purchased from Beijing 4A Biotech Co., Ltd. (Beijing, China).

Plant Materials. The *R. beesianus* rhizomes, identified by Mr. Buyun Zhang, were purchased from Dali City of Yunnan province, China, on January 25, 2018, kept dry, and ventilated. A voucher specimen (no. 20180125) was stored in a cool and dried environment of Kunming Institute of Botany, CAS.

Extraction and Isolation. The air-dried *R. beesianus* rhizomes (8.0 kg) were kibbled and extracted with 90% aqueous EtOH (50 L × 4, each time for 3 h), and then the solvent was evaporated in vacuum. The extract (622 g) was chromatographed on a silica gel column using sequential gradient elution of CHCl₃–Me₂CO (1:0–0:1) to obtain six fractions. Fraction II (23.9 g) was separated on a YMC column, eluted successively with MeOH/H₂O (75:25–100:0), and then purified on a silica gel column (petroleum ether–Me₂CO, 30:1–20:1) to give compounds **12** (14.4 mg), **14** (212.3 mg), and **8** (11.2 mg). Fraction IV (15.8 g) was applied on an MCI column, eluted successively with MeOH/H₂O (40:60–100:0), and then chromatographed over a silica gel column elution with CHCl₃/Me₂CO (10:1) to obtain **13** (4.5 mg). Fraction V (114 g) was subjected to an RP-C₁₈ column with a gradient of MeOH/H₂O (30:70–85:15) to afford five subfractions V-1 to V-5. Subfraction V-1 (12.4 g) was chromatographed on a silica gel column (CHCl₃/MeOH, 8:1) to get compound **10** (279.1 mg) and a mixture. The latter was further separated over HPLC to give **11** (15.8 mg; *t_R* = 12 min; CH₃CN/H₂O, 7:93; 3.0 mL/min). Subfraction V-3 (11 g) was separated on a silica gel column (CHCl₃/MeOH, 20:1) and then purified over HPLC to yield compounds **1** (8.5 mg; *t_R* = 40.5 min; CH₃CN/H₂O, 35:65; 1.0 mL/min), **2** (7.3 mg; *t_R* = 43.5 min; CH₃CN/H₂O, 35:65; 1.0 mL/min), and **15** (8.1 mg; *t_R* = 27.5 min; CH₃CN/H₂O, 40:60; 1.0 mL/min). Subfraction V-4 (20.5 g) was separated on a silica gel column (CHCl₃/MeOH, 20:1–6:1) to give compound **7** (15.3 mg) and a mixture, which was purified by HPLC to afford compound **9** (9.6 mg; *t_R* = 52 min; MeOH/H₂O, 25:75; 2.5 mL/min). Subfraction V-5 (13.8 g) was subjected on a silica gel column (CHCl₃–MeOH, 6:1–2:1) to afford compounds **6** (113.0 mg) and **4** (24.5 mg) and subfractions V-5-1 to V-5-3. Subfraction V-5-1 was separated on a silica gel column (CHCl₃/MeOH, 6:1) and then isolated on a Sephadex LH-20 column with MeOH to obtain **3** (6.8 mg). Subfraction V-5-2 was applied on a silica gel column (CHCl₃/MeOH, 6:1) and then isolated on a Sephadex LH-20 column (MeOH) to yield **5** (8.9 mg) (Figure 1).

Acid Hydrolysis of Compounds 3 and 9 and HPLC Analysis. The acid hydrolysis of compounds **3** and **9** was carried out by a previously reported procedure, with minor modifications.²³ Compound **3** (2.0 mg) was refluxed with 2 mL of solvents (2 M TFA) on an oil bath for 2 h at 120 °C. Then, the aglycone was extracted with CHCl₃ (1 mL, three times). Next, 60 μL of NaOH (0.3 mol/L) and 60 μL of PMP (0.5 mol/L in methanol) were added to derivatize the sugar in the aqueous portion and reacted at 75 °C for 60 min. Then, the reaction was quenched with 60 μL of HCl (0.3 mol/L) and the reaction mixture was extracted with CHCl₃ (1 mL, three times). The aqueous layer was further analyzed over HPLC (*t_R* = 18.5 min; 18% acetonitrile:82% sodium phosphate (pH 6.8); 1.5 mL/min). The acid hydrolysis and HPLC analysis of **9** were performed by the same way as that of **3**. Likewise, the standard monosaccharide D-Glc (1 mg) was derivatized with PMP the same way as **3** and **9**, and HPLC analysis was performed under the same conditions as **3** and **9**. The sugar moieties of compounds **3** and **9** were identified as D-Glc, showing retention times (*t_R* = 18.5 min) consistent with the standard monosaccharide (D-glucose) derivative.

ECD Calculations. The ECD calculations of **3a** (the aglycone of compound **3**) were achieved using Gaussian 16. More specifically, the 3D structure of **3a** was first confirmed by its ROESY spectrum and then passed to conformational analysis, which was applied for CONFLEX software (Conflex Corp., Tokyo, Japan) including a molecular mechanics force field (MMFF94s). At the B3LYP/6-31+G(d) level in the gas phase, the available conformers were further optimized by the density functional theory (DFT). Using time-dependent DFT (TDDFT) at the B3LYP/6-311+G(d) level, ECD calculations were used for the optimized conformations, and finally,

the calculated ECD curves were obtained by SpecDis version 1.63 software.²⁴

Preparation of the (R)- and (S)-MTPA Ester Derivatives of Compound 9a. Mosher's reaction was performed in accordance with the previous method with slight modifications.²⁵ Compound **9a** (the aglycone of compound **9**) (1 mg) was dissolved in 500 μL of anhydrous tetrahydrofuran (THF), and then 2 equiv of 4-(dimethylamino) pyridine (4-DMAP), 2 equiv of DCC, and 2 equiv of (R)-MTPA chloride were added under vacuum. The mixture was dried and stirred at 25 °C for 24 h. Then, the solvent was removed, the mixture was purified using a Sephadex LH-20 column (MeOH), and the (R)-MTPA ester of **9aR** was obtained. The (S)-MTPA ester of compound **9aS** was prepared by the same procedure. The ¹H NMR spectra of the (R)- and (S)-MTPA esters were obtained after each reaction.

Rhynchanine A (1). White amorphous powder; $[\alpha]_{\text{D}}^{22}$ –28.6° (c 0.17, MeOH); UV (MeOH) λ_{max} (log ϵ) 196 (3.9), 244 (4.0), 268 (4.2) nm; IR (KBr) ν_{max} 3439, 2922, 1614, 1514, 1266, 1224, 1033, 816 cm⁻¹; ¹H NMR (CD₃OD, 600 MHz) and ¹³C NMR (CD₃OD, 150 MHz) data, see Table 1; positive HRESIMS *m/z* 723.3142 [M + Na]⁺ (calcd. for C₄₁H₄₈O₁₀Na⁺, 723.3140).

Rhynchanine B (2). White amorphous powder; $[\alpha]_{\text{D}}^{22}$ –21.2° (c 0.25, MeOH); UV (MeOH) λ_{max} (log ϵ) 196 (4.8), 244 (4.0), 267 (4.2) nm; IR (KBr) ν_{max} 3431, 2923, 1614, 1514, 1265, 1225, 1033, 820 cm⁻¹; ¹H NMR (CD₃OD, 600 MHz) and ¹³C NMR (CD₃OD, 150 MHz) data, see Table 1; positive HRESIMS *m/z* 723.3145 [M + Na]⁺ (calcd. for C₄₁H₄₈O₁₀Na⁺, 723.3140).

Rhynchanine C (3). White amorphous powder; $[\alpha]_{\text{D}}^{26}$ –14.9° (c 0.10, MeOH); UV (MeOH) λ_{max} (log ϵ) 196 (3.7), 264 (3.1), 308 (3.1), 337 (3.2) nm; IR (KBr) ν_{max} 3417, 2920, 1637, 1614, 1518, 1276, 1076, 1034 cm⁻¹; ¹H NMR (DMSO-*d*₆, 600 MHz) and ¹³C NMR (DMSO-*d*₆, 150 MHz) data, see Table 2; positive HRESIMS *m/z* 591.2048 [M + Na]⁺ (calcd. for C₂₇H₃₆O₁₃Na⁺, 591.2048).

Tsaokopyranol G (3a). White amorphous powder; $[\alpha]_{\text{D}}^{23}$ –19.5° (c 0.032, MeOH); ¹H NMR (CD₃OD, 400 MHz) δ_{H} : 7.09 (1H, s, H-2'), 6.90 (1H, s, H-2''), 6.68–6.77 (4H, overlap, H-5', 6', 5'', 6''), 4.80 (1H, d, *J* = 6.8 Hz, H-7), 4.55 (1H, d, *J* = 11.3 Hz, H-1), 4.26 (1H, m, H-3), 3.93 (3H, s, 3'-OCH₃), 3.72 (3H, s, 5'-OCH₃), 3.64 (1H, m, H-5), 3.43 (1H, dd, *J* = 8.0, 1.9 Hz, H-6), 2.07 (1H, t, *J* = 13.2 Hz, H-4a), 1.81 (1H, d, *J* = 14.0 Hz, H-2a), 1.73 (1H, q, *J* = 12.2 Hz, H-2b), 1.47 (1H, d, *J* = 14.1 Hz, H-4b).

4-O-methylstroside B (9). White amorphous powder; $[\alpha]_{\text{D}}^{21}$ +16.2° (c 0.07, MeOH); UV (MeOH) λ_{max} (log ϵ) 197 (4.4), 252 (2.7), 278 (3.2) nm; IR (KBr) ν_{max} 3424, 2924, 1631, 1516, 1262, 1075, 1027 cm⁻¹; ¹H NMR (DMSO-*d*₆, 500 MHz) and ¹³C NMR (DMSO-*d*₆, 125 MHz) data, see Table 2; positive HRESIMS *m/z* 397.1468 [M + Na]⁺ (calcd. for C₁₇H₂₆O₉Na⁺, 397.1469).

(R)-3-(3-(4-Dimethoxyphenyl)propane-1,2-diol (9a). White amorphous powder; $[\alpha]_{\text{D}}^{23}$ +35.1° (c 0.043, MeOH); ¹H NMR (CD₃OD, 400 MHz) δ_{H} : 6.77 (1H, d, *J* = 8.2 Hz, H-5), 6.75 (1H, d, *J* = 2.0 Hz, H-2), 6.68 (1H, dd, *J* = 8.2, 2.0 Hz, H-6), 3.73 (3H, s, 3-OCH₃), 3.70 (3H, s, 4-OCH₃), 3.67 (1H, overlap, H-8), 3.37 (2H, dd, *J* = 11.1, 5.4 Hz, H-9), 2.67 (1H, dd, *J* = 13.8, 5.6 Hz, H-7a), 2.52 (1H, dd, *J* = 13.8, 7.5 Hz, H-7b).

Antioxidant Activity Assays. DPPH Radical Scavenging Activity. The DPPH scavenging capacity of the compounds was carried out by a previous method with slight modifications.^{26,27} Briefly, 50 μL of the sample (12.5, 25, 50, 75, and 100 μM) and 200 μL of DPPH (0.1 mM in 95% ethanol) were put in a 96-well plate and measured as (A_x). The blank contained 50 μL of the sample (12.5, 25, 50, 75, and 100 μM) and 200 μL of 95% ethanol and was measured as (A_{x0}), while the control included 50 μL of ethanol and 200 μL of DPPH (0.1 mM in 95% ethanol) and was observed as (A₀). All the mixtures were shaken thoroughly at 30 °C for half an hour in the dark, and then the absorbance values were recorded later (at 517 nm). The

Table 1. ^1H (600 MHz) and ^{13}C NMR (150 MHz) Spectroscopic Data for 1 and 2 in CD_3OD

position	1		2	
	δ_{H} (mult., J in Hz)	δ_{C}	δ_{H} (mult., J in Hz)	δ_{C}
1	4.72 d (9.7)	77.8	4.71 d (9.7)	77.9
2	4.15 dd (9.7, 2.8)	84.0	4.14 dd (9.7, 2.9)	83.9
3	4.30 m	66.7	4.28 m	66.7
4	1.95 ddd (14.1, 3.7, 2.1)	39.1	1.94 ddd (14.2, 3.7, 2.0)	39.0
	1.75 overlap		1.74 overlap	
5	3.95 m	72.4	3.96 m	72.4
6	1.79 m	38.9	1.78 m	38.9
	1.70 overlap		1.69 overlap	
7	2.62 m	32.1	2.56 m	32.2
1'		132.7		133.2
2'	7.00 d (2.0)	112.8	6.98 d (1.9)	112.8
3'		148.8		148.8
4'		147.8		148.0
5'	6.76 d (8.1)	115.9	6.74 d (8.1)	115.9
6'	6.93 dd (8.1, 2.0)	122.2	6.91 dd (8.1, 1.9)	122.2
3'-OMe	3.78 s	56.5	3.77 s	56.5
1''		134.3		134.2
2''	6.96 d (8.5)	130.4	6.98 d (8.5)	130.4
3''	6.64 d (8.5)	116.2	6.66 d (8.5)	116.3
4''		156.6		156.7
5''	6.64 d (8.5)	116.2	6.66 d (8.5)	116.3
6''	6.96 d (8.5)	130.4	6.98 d (8.5)	130.4
1'''	6.47 d (15.9)	134.3	6.42 d (15.9)	133.2
2'''	5.86 dd (15.9, 8.3)	129.3	5.91 dd (15.9, 8.0)	129.9
3'''	3.90 td (8.3, 7.0)	82.4	3.93 td (8.5, 3.7)	80.8
4'''	1.83 dd (7.0, 2.1)	44.1	1.73 overlap	45.0
	1.64 m		1.56 ddd (14.2, 9.0, 3.7)	
5'''	3.62 td (8.5, 4.4)	69.3	3.75 overlap	68.2
6'''	1.68 m	41.0	1.66 m	41.3
7'''	2.53 m	32.2	2.64 m	32.1
3'''-OMe	3.26 s	56.4	3.27 s	56.7
1''''		133.3		133.4
2''''	6.93 d (2.0)	111.4	6.95 d (2.0)	111.4
3''''		152.4		152.4
4''''		148.3		148.3
5''''	6.51 d (8.3)	120.2	6.50 d (8.3)	120.2
6''''	6.77 dd (8.3, 2.0)	120.9	6.76 dd (8.3, 2.0)	120.8
3''''-OMe	3.79 s	56.6	3.78 s	56.6
1'''''		134.3		134.3
2'''''	6.99 d (8.5)	130.5	6.99 d (8.5)	130.5
3'''''	6.68 d (8.5)	116.3	6.67 d (8.5)	116.3
4'''''		156.6		156.6
5'''''	6.68 d (8.5)	116.3	6.67 d (8.5)	116.3
6'''''	6.99 d (8.5)	130.5	6.99 d (8.5)	130.5

DPPH radical scavenging activity (RSA) of the samples was calculated by the following formula:

$$\text{RSA} (\%) = \frac{A_0 - (A_x - A_{x0})}{A_0} \times 100\%$$

The positive control was ascorbic acid (V_C), and all data were the averages of triplicate measurements.

ABTS Radical Scavenging Activity. To find out the antioxidant capacity of the samples, the ABTS assay was carried out with an improved method as reported previously.²⁷ In short, the working solution (ABTS⁺ solution) was diluted to an absorbance of 0.70 ± 0.02 when measured at 734 nm. The test mixture consisting of 25 μL

of the sample (12.5, 25, 50, 75, and 100 μM) and 200 μL of ABTS⁺ solution was taken in a 96-well plate and measured as (A_x). The blank contained 25 μL of the sample (12.5, 25, 50, 75, and 100 μM) and 200 μL of 95% ethanol and was measured as (A_{x0}), while the control included 25 μL of ethanol and 200 μL of ABTS⁺ solution and was observed as (A_0). All the mixtures were shaken thoroughly at 30 $^\circ\text{C}$ in the dark for 6 min, and then the absorbance values were tested later (at 734 nm). All the solutions were prepared on the same day for the assay. The antioxidant activity (RSA) of all samples was calculated as follows:

$$\text{RSA} (\%) = \frac{A_0 - (A_x - A_{x0})}{A_0} \times 100\%$$

The positive control was ascorbic acid (V_C), and all data were the averages of triplicate measurements.

Ferric Reducing Antioxidant Power (FRAP) Assay. The FRAP assay was assessed by a previously reported procedure with minor modifications.²⁷ The acetate buffer (300 mM, pH 3.6) and tripyridyltriazine solution (10 mM) in 40 mM HCl were mixed with $\text{FeCl}_3 \cdot 6\text{H}_2\text{O}$ (20 mM) in proportion of 10:1:1, and then the resultant FRAP reagent was kept in a water bath for 0.5 h at 37 $^\circ\text{C}$. The test mixtures including 20 μL of the sample (12.5, 25, 50, 75, and 100 μM) and 180 μL of FRAP reagent were kept in a 96-well plate and measured as (A_x). The blank contained 200 μL of 95% ethanol and 20 μL of distilled water and was measured as (A_{x0}). All the mixtures were kept at 37 $^\circ\text{C}$ in the dark for 10 min, and then the absorbance values were taken later (at 593 nm). Ferrous sulfate ($\text{FeSO}_4 \cdot 7\text{H}_2\text{O}$) was used to protract the standard curve ($y = 1.3334x + 0.08$). All the solutions were prepared freshly before use.

Intracellular Antioxidant Capacity against H_2O_2 -Induced HepG-2 Cells. Cell Culture and MTT Assay. HepG-2 cells were obtained from Kunming Cell Bank, CAS, and maintained in DMEM medium using 10% (v/v) fetal bovine serum (FBS), supplemented with 1% antibiotics, which were a mixture of penicillin (100 U/mL) and streptomycin (100 mg/mL), and then cultured in a humidified environment containing 5% $\text{CO}_2/95\%$ air at 37 $^\circ\text{C}$. The viability of the cells was tested by MTT assay in accordance with a reported method.²⁸ The HepG-2 cells were seeded in a 96-well plate (5000 cells/well) and then cultured overnight. After treating with different concentrations of compounds (2.5, 5, 10, 20, and 40 μM) and enduring for 6 h, 20 μL of MTT (5 mg/mL) was added to the wells, and then the cells were cultured at 37 $^\circ\text{C}$ for another 4 h. At last, the culture medium was discarded, and then DMSO (100 μL) was added to thoroughly dissolve the blue crystals in each well. The absorbance was subsequently measured at 570 nm.

Assessment of Intracellular Reactive Oxygen Species (ROS). A fluorescence DCFH-DA probe was used to quantify the intracellular ROS content according to the reported instructions.^{2,27} HepG-2 cells were seeded in six-well plates (2×10^5 cells/well) and were cultured for 24 h. Then, compounds 1–8 (10 μM) or V_C (10 μM , positive control) was used to treat the cells for another 24 h. The cells were collected and washed with cold PBS, then 0.7 mM H_2O_2 was added, and the cells were incubated for another 6 h. After that, the culture medium was discarded, serum-free medium and 1 mL of 10 μM DCFH-DA were added, and then the cells were cultured in the dark at 37 $^\circ\text{C}$. After incubating for 20 min, the cells were washed and detected with flow cytometry.

Assessment of Cytoprotective Activity against H_2O_2 -Induced HepG-2 Cell Apoptosis. Apoptotic and necrotic cells were monitored using the Annexin V-FITC/PI detection kit in line with a previous study with slight modifications.¹ HepG-2 cells were incubated and treated with the compounds. Subsequently, the cells were collected, washed with cold PBS, and then resuspended in 100 μL of buffer. After staining the cells with Annexin V-FITC (5 μL) at room temperature for 5 min, the cells were stained with 10 μL of PI (20 $\mu\text{g}/\text{mL}$) and reacted for 5 min in an ice bath. Afterward, the percentage of apoptosis and necrosis of HepG-2 cells was analyzed by flow cytometry (BD Biosciences, USA).

Table 2. ^1H and ^{13}C NMR Spectroscopic Data for 3, 5, and 9^a in DMSO-*d*₆

position	3		5		position	9	
	δ_{H} (mult., <i>J</i> in Hz)	δ_{C}	δ_{H} (mult., <i>J</i> in Hz)	δ_{C}		δ_{H} (mult., <i>J</i> in Hz)	δ_{C}
1	4.58 dd (11.5, 3.3)	73.1	7.56 d (15.8)	142.6	1		132.0
2	1.74 ddd (13.8, 3.3, 2.8)	39.2	7.09 d (15.8)	122.6	2	6.85 d (1.9)	113.7
	1.54 ddd (13.8, 11.5, 2.8)				3		148.8
3	4.09 m	62.7		188.4	4		147.5
4	1.67 ddd (14.4, 11.4, 2.8)	33.6	6.63 d (15.2)	124.5	5	6.84 d (8.1)	112.1
	1.44 ddd (14.4, 3.1, 2.8)				6	6.74 dd (8.1, 1.9)	121.6
5	4.10 overlap	71.5	7.50 d (15.2)	143.9	7	2.71 dd (13.6, 5.7)	39.4
6	3.69 dd (5.6, 3.6)	82.3	7.00 d (15.2)	128.4		2.54 dd (13.6, 7.3)	
7	4.74 d (5.6)	71.9	6.97 d (15.2)	142.3	8	3.80 m	70.9
1'		134.0		126.2	9	3.68 dd (10.0, 4.2)	73.5
2'	6.91 d (1.9)	110.5	6.99 d (1.9)	114.3		3.27 dd (10.0, 6.7)	
3'		147.2		146.0	3-OMe	3.73 s	55.9
4'		145.5		147.7	4-OMe	3.71 s	55.8
5'	6.72 d (8.1)	115.0	6.76 d (8.1)	116.3	1''	4.13 d (7.7)	103.9
6'	6.75 dd (8.1, 1.9)	118.3	6.89 dd (8.1, 1.9)	120.4	2''	2.99 t (7.8)	74.0
3''-OMe	3.76 s	55.6			3''	3.08 m	77.3
1''		133.8		128.2	4''	3.06 m	70.4
2''	6.97 d (1.9)	111.7	7.62 d (8.4)	130.9	5''	3.14 t (8.6)	76.8
3''		146.9	6.83 d (8.4)	116.3	6''	3.64 dd (11.7, 1.8)	61.4
4''		145.2		160.3		3.43 dd (11.7, 5.3)	
5''	6.68 d (8.1)	114.7	6.83 d (8.4)	116.3			
6''	6.78 dd (8.1, 1.9)	119.5	7.62 d (8.4)	130.9			
3'''-OMe	3.70 s	55.3					
1'''	4.33 d (7.7)	101.9					
2'''	2.99 m	73.5					
3'''	3.04 dd (17.1, 8.6)	77.0					
4'''	3.14 dd (17.1, 8.6)	70.1					
5'''	3.42 overlap	76.4					
6'''	3.67 dd (11.7, 1.8)	61.4					
	3.43 overlap						

^aCompounds 3 and 5 were measured at ^1H (600 MHz) and ^{13}C NMR (150 MHz); compound 9 was measured at ^1H (500 MHz) and ^{13}C NMR (125 MHz).

RESULTS AND DISCUSSION

Structure Elucidation of Purified Compounds 1–3 and 9.

Compound 1 was obtained as a white amorphous powder. Its molecular formula was assigned on $\text{C}_{41}\text{H}_{48}\text{O}_{10}$ on the basis of the positive HRESIMS ion at m/z 723.3142 [$\text{M} + \text{Na}$]⁺ (calcd. for $\text{C}_{41}\text{H}_{48}\text{O}_{10}\text{Na}^+$, 723.3140), indicating 18 degrees of unsaturation. The ^1H NMR spectrum (Table 1) showed the presence of two AA'BB' systems (δ_{H} 6.64 and 6.96, each d, $J = 8.5$ Hz; δ_{H} 6.68 and 6.99, each d, $J = 8.5$ Hz) and two ABX systems (δ_{H} 6.76, d, $J = 8.1$ Hz; 6.93, dd, $J = 8.1, 2.0$ Hz; 7.00, d, $J = 2.0$ Hz; and δ_{H} 6.51, d, $J = 8.3$ Hz; 6.77, dd, $J = 8.3, 2.0$ Hz; 6.93, d, $J = 2.0$ Hz), which suggested the presence of two 1,4-disubstituted and two 1,3,4-trisubstituted phenyl groups.²⁹ Moreover, the ^1H NMR spectrum of 1 displayed resonance signals for a pair of olefinic protons, three methoxy groups, and six oxygenated methine protons (Table 1). The ^{13}C NMR spectrum displayed 41 carbon signals, including three methoxy groups, six aliphatic methylenes, six oxygenated methine groups, and 26 aromatic carbon resonances (16 methines and 10 quaternary carbons, including four benzene rings and a double bond) (Table 1). These data suggested that 1 was a diarylheptanoid dimer with two C6–C7–C6 units,³⁰ corresponding to the structures similar to hedycoropyran B (unit I)³¹ and neohexahydrocurcumin (unit II)³² (Figure 1).

The long-range ^1H – ^1H COSY connectivity of δ_{H} 2.62 (H-7)/1.79 (H-6)/3.95 (H-5)/1.95 (H-4)/4.30 (H-3)/4.15 (H-2)/4.72 (H-1) and the HMBC correlations from δ_{H} 4.72 (1H, d, $J = 9.7$ Hz, H-1) to δ_{C} 132.7 (s, C-1'), 112.8 (d, C-2'), 122.2 (d, C-6'), and 72.4 (d, C-5) and from δ_{H} 3.95 (1H, m, H-5) to δ_{C} 77.8 (d, C-1), 66.7 (d, C-3), and 32.1 (t, C-7) presented a heptane chain having a tetrahydropyran ring linking C-1 to C-5 in unit I of 1 (Figure 2). Meanwhile, the other long-range ^1H – ^1H COSY connectivity of H-7''' (δ_{H} 2.53) and H-1''' (δ_{H} 6.47) to the adjacent protons and the chemical shifts of C-1''' (δ_{C} 134.3, d), C-2''' (δ_{C} 129.3, d), C-3''' (δ_{C} 82.4, d), and C-5''' (δ_{C} 69.3, d) confirmed the other heptane chain with a double bond and two oxygenated methines in unit II of 1. The unit I of 1 was similar to hedycoropyran B except the absence of a hydroxyl group at C-6, which was suggested by HMBC correlations of δ_{H} 1.79 (1H, m, H-6) with δ_{C} 39.1 (t, C-4) and 134.3 (s, C-1'') and the chemical shift of C-6 (δ_{C} 38.9, t). Meanwhile, the unit II of 1 resembled neohexahydrocurcumin with the exception of an additional methoxy group at C-3''' and the absence of a methoxy group C-3''', as confirmed by HMBC correlations of δ_{H} 3.26 (3H, s) with δ_{C} 82.4 (d, C-3''') and of δ_{H} 6.99 (2H, d, $J = 8.5$ Hz, H-2'''' and 6''''') to δ_{C} 156.6 (s, C-4'''''). The other two methoxy groups were located at C-3' and C-3''', which were supported by HMBC correlations from δ_{H} 3.78 (3H, s) to δ_{C} 148.8 (s, C-3') and from δ_{H} 3.79 (3H, s) to δ_{C} 152.4 (s, C-3'''), respectively. Finally, the HMBC

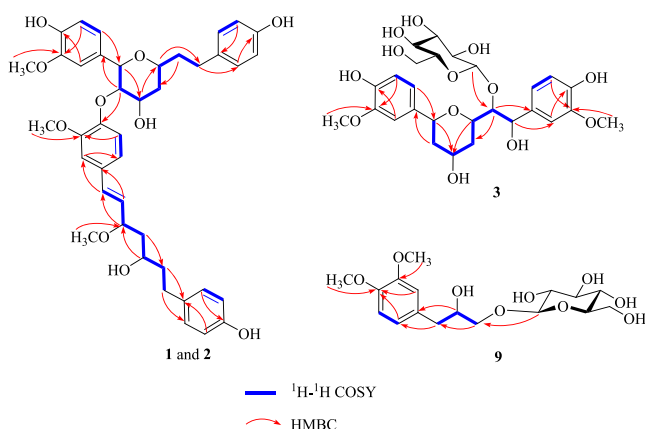


Figure 2. Key ^1H – ^1H COSY and HMBC correlations of compounds 1–3 and 9.

correlation from δ_{H} 4.15 (1H, dd, $J = 9.7, 2.8$ Hz, H-2) to δ_{C} 148.3 (s, C-4 $'''$) implied that the two units were connected via an ether linkage between C-2 and C-4 $'''$.^{30,31} Thus, the planar structure of compound 1 was elucidated and named as rhynchanine A.

The ROESY correlation of H-1 with H-5, of H-2 with H-3 and H $_{\text{ax}}$ -4, and of H-3 with H $_{\text{ax}}$ -4 (Figure 3) indicated that the tetrahydropyran ring of unit I of 1 was in a chair conformation and H-1 and H-5 were in an axial orientation.^{31,33} The $J_{1,2} = 9.7$ Hz and $J_{2,3} = 2.8$ Hz values indicated that H-1 and H-2 were in an axial orientation and H-3 was in an equatorial orientation, as confirmed by ROESY correlations of H-1 with H-2 $'''$. The large coupling constants ($J = 15.9$ Hz) between H-1 $'''$ and H-2 $'''$ suggested an *E* configuration of the double bond. Although the ROESY correlation of H-3 $'''$ with H-5 $'''$ could be obviously observed, the configurations of H-3 $'''$ and H-5 $'''$ could not be determined because of the flexible heptane chain in unit II of 1.

The molecular formula of 2 was established as $\text{C}_{41}\text{H}_{48}\text{O}_{10}$ by the positive HRESIMS spectrum ($[\text{M} + \text{Na}]^+$ at m/z 723.3145), which was similar to that of 1. They had the same physical data in the UV and IR spectra, suggesting the presence of the same functional groups. The 1D and 2D NMR spectra of 2 showed almost the same behavior to those of 1 (Table 1), except that the chemical shifts of C-3 $'''$ and C-5 $'''$ in 2 slightly shifted ($\Delta\delta_{\text{H}}$ +0.03 ppm and +0.13 ppm and $\Delta\delta_{\text{C}}$ –1.6 ppm and –1.1 ppm, respectively), compared with those of C-3 $'''$ and C-5 $'''$ in 1. Therefore, compound 2 was elucidated

as the diastereomer of 1 at C-3 $'''$ and/or C-5 $'''$ and named as rhynchanine B.

Structurally, compounds 1 and 2 had two chiral carbons with uncertain configuration (C-3 $'''$ and C-5 $'''$), and the possible relative configurations of C-3 $'''$ and C-5 $'''$ were 3 $'''R$ 5 $'''R$, 3 $'''S$ 5 $'''S$, 3 $'''R$ 5 $'''S$, and 3 $'''S$ 5 $'''R$. Thus, compounds 1 and 2 were two of four diastereomers and were isolated as highly pure monomers, which were supported by 1D and 2D NMR data. To determine the absolute configuration, the *para*-toluene sulfonyl ester derivatives of 1 and 2 were synthesized to grow their crystals. Unfortunately, the crystals were not formed. Moreover, the experimental electron circular dichroism (ECD) and calculated curves did not coincide because of the flexible heptane chain in unit II of 1 and 2.

The molecular formula of 3 was determined as $\text{C}_{27}\text{H}_{36}\text{O}_{13}$ by the molecular ion peak at m/z 591.2048 $[\text{M} + \text{Na}]^+$ in the HRESIMS, suggesting 10 degrees of unsaturation. The ^1H NMR spectrum (Table 2) showed that 3 had resonances for six aromatic protons at δ_{H} 6.68 (1H, d, $J = 8.1$ Hz), 6.78 (1H, dd, $J = 8.1, 1.9$ Hz), 6.97 (1H, d, $J = 1.9$ Hz), 6.72 (1H, d, $J = 8.1$ Hz), 6.75 (1H, dd, $J = 8.1, 1.9$ Hz), and 6.91 (1H, d, $J = 1.9$ Hz), presenting two 1,3,4-trisubstituted benzene rings.²⁹ An anomeric proton at δ_{H} 4.33 (1H, d, $J = 7.7$ Hz), an oxygenated methylene group at δ_{H} 3.67 (1H, dd, $J = 11.7, 1.8$ Hz) and 3.43 (1H, overlapped), along with five oxygenated methine carbons at δ_{C} 101.9, 77.0, 76.4, 73.5, and 70.1, and an oxygenated methylene carbon at δ_{C} 61.4 indicated that a β -glucose moiety was present in 3. The sugar unit was identified as *D*-glucose ($t_{\text{R}} = 20.5$ min) by acid hydrolysis and HPLC analysis.²³ Besides the β -*D*-glucose moiety and two 1,3,4-trisubstituted benzene rings, there were signals for five oxygenated methine groups in the ^{13}C NMR spectrum.^{33,34} Comparison of NMR spectroscopic data of 3 indicated that its aglycone resembled tsaokopyranol G, except that the major difference was one more β -*D*-glucose moiety in 3.³⁵ The β -*D*-glucose moiety was attached at C-6 of the aglycone via an ether linkage, as supported by the HMBC correlations from H-1 $'''$ to δ_{C} 82.3 (d, C-6).

The ROESY correlation of H-1 with H-5, of H-2 with H-3 and H $_{\text{ax}}$ -4, and of H-3 with H $_{\text{ax}}$ -4 (Figure 3) indicated that the tetrahydropyran ring of unit I of 1 was in a chair conformation and H-1 and H-5 were in an axial orientation.^{31,33} Two protons [δ_{H} 1.74 (ddd, $J = 13.8, 3.3, 2.8$ Hz) and 1.54 (ddd, $J = 13.8, 11.5, 2.8$ Hz)] were linked to C-2; the former should be equatorial and the latter should be axial. Meanwhile, the proton at δ_{H} 1.67 (ddd, $J = 14.4, 11.4, 2.8$ Hz, H-4) should be

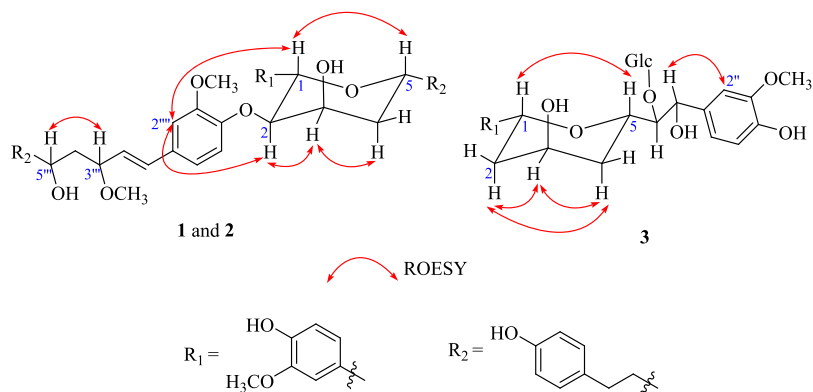


Figure 3. Key ROESY correlations of compounds 1–3.

axial and the other proton at δ_{H} 1.44 (ddd, $J = 14.4, 3.1, 2.8$ Hz, H-4) should be equatorial. The $J_{1,2} = 11.5$ Hz, $J_{2,3} = 2.8$ Hz, and $J_{3,4} = 3.1$ Hz values indicated that H-1, $\text{H}_{\text{ax}-2}$, and $\text{H}_{\text{ax}-4}$ were axially oriented and H-3 was in an equatorial orientation, as supported by the ROESY correlations of $\text{H}_{\text{ax}-2}$ with $\text{H}_{\text{ax}-4}$ and of $\text{H}_{\text{ax}-2}/\text{H}_{\text{ax}-4}$ with H-3. To assign the absolute configurations, the hydrolysis of **3** afforded the aglycone (compound **3a**) and a sugar unit, and the absolute configuration of **3a** was determined as 1*R*,3*S*,5*S*,6*S*,7*R* by the ECD calculations, which showed a high agreement between the experimental and calculated ECD spectra (Figure 4). Thus, the structure of **3** was determined and named rhynchanine C.

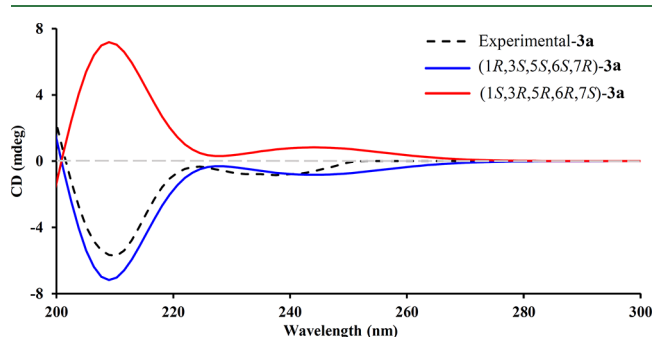


Figure 4. Experimental and calculated ECD of compound **3a** (the aglycone of compound **3**).

Compound **9** was isolated as a white amorphous powder. It possessed a molecular formula of $\text{C}_{17}\text{H}_{26}\text{O}_9$ as established by its HRESIMS ion at m/z 397.1468 $[\text{M} + \text{Na}]^+$. The ^1H NMR spectrum (Table 2) showed the presence of a 1,3,4-trisubstituted benzene ring.³⁰ An anomeric proton signal at δ_{H} 4.13 (1H, d, $J = 7.7$ Hz), five oxygenated methine carbons at δ_{C} 103.9, 77.3, 76.8, 74.5, and 70.4 and an oxygenated methylene carbon at δ_{C} 61.4 indicated the presence of a β -glucose moiety in **9**. The sugar unit was identified as D-glucose using the same method as for **3**.²³ Detailed analysis of the ^1H and ^{13}C NMR spectra of **9** showed that these were similar to that of stroside B,³⁶ except for a methoxy group at C-4 in **9** instead of a hydrogen in stroside B, which was indicated by

HMBC correlations from δ_{H} 3.73 (3H, s) to δ_{C} 147.5 (s, C-4). The β -D-glucose moiety was attached at C-9 as indicated by HMBC correlations from H-1'' to δ_{C} 73.5 (d, C-9). The optical rotation value ($[\alpha]_{\text{D}}^{21} +16.2^\circ$) was in good agreement with that of stroside B ($[\alpha]_{\text{D}}^{25} +8.0^\circ$), which suggested that the absolute configuration of C-8 was *R*.³⁶ To confirm the surmise, the hydrolysis of **9** afforded the aglycone (compound **9a**) and a sugar unit, and the optical rotation value of compound **9a** ($[\alpha]_{\text{D}}^{23} +35.1^\circ$) was in good agreement with that of (+)-3-(3,4-dimethoxyphenyl)propane-1,2-diol ($[\alpha]_{\text{D}}^{26} +18^\circ$), while the optical rotation value of the (−)-isomer was the opposite ($[\alpha]_{\text{D}}^{26} -23^\circ$), which further verified that the absolute configuration of C-8 was *R*.³⁷ In addition, Mosher's ester was also synthesized from the aglycone (compound **9a**) to determine the absolute configuration of C-8. Treatment with (*R*)- and (*S*)-MTPA chlorides led to esterification of the OH-8 group to afford the (*S*)- and (*R*)-MTPA derivatives, respectively. Unfortunately, in the ^1H NMR spectra, there was no difference in the chemical shifts between (*R*)-MTPA ester and (*S*)-MTPA ester; it might be due the influence of 9-OH.²⁵ Consequently, the structure of **9** was determined and named as 4-*O*-methylstroside B.

Eleven known compounds were identified as plantagineoside C (**4**),³² 7-(3,4-di-hydroxyphenyl)-1-(4-hydroxyphenyl)-1,4,6-heptatrien-3-one (**5**),²² 3,5-dihydroxy-1-(3,4-dihydroxyphenyl)-7-(4-hydroxyphenyl)-heptane (**6**),³⁸ pinoselinol (**7**),³⁹ kaempferol (**8**),⁴⁰ citrulin C (**10**),⁴¹ tachioside (**11**),⁴² 3,4-dimethoxycinnamaldehyde (**12**),⁴³ 3-methoxy-4-hydroxycinnamaldehyde (**13**),³⁹ eugenol (**14**),⁴⁴ and 4-hydroxy-benzalacetone (**15**)⁴⁵ by comparison with the previously reported data in the literature (Figures S50–S71, Supporting Information).

Antioxidant Activities In Vitro. The antioxidant capacity of compounds (**1**–**15**) was assessed by DPPH, ABTS⁺, and FRAP assays (Table 3). In the DPPH assay, compounds **4** ($\text{SC}_{50} = 18.41 \pm 1.27 \mu\text{M}$), **3** ($\text{SC}_{50} = 19.25 \pm 1.28 \mu\text{M}$), and **6** ($\text{SC}_{50} = 25.86 \pm 1.41 \mu\text{M}$) showed a stronger efficiency as compared with ascorbic acid ($\text{SC}_{50} = 29.81 \pm 1.474 \mu\text{M}$). In

Table 3. Antioxidant Activity of Compounds **1**–**15** from *R. beesianus*^e

sample	DPPH ^{a,b}	ABTS ^{a,b}	FRAP ^{a,c}
rhynchanine A (1)	29.96 ± 1.26	32.26 ± 1.24	2446.54 ± 41.63
rhynchanine B (2)	29.88 ± 1.26	33.18 ± 1.24	2146.59 ± 61.09
rhynchanine C (3)	19.25 ± 1.28	31.26 ± 1.50	1699.25 ± 55.58
plantagineoside C (4)	18.41 ± 1.27	35.17 ± 1.55	2399.88 ± 119.99
7-(3,4-di-hydroxyphenyl)-1-(4-hydroxyphenyl)-1,4,6-heptatrien-3-one (5)	30.65 ± 1.49	118.25 ± 2.01	2573.21 ± 162.88
[(3 <i>R</i> ,5 <i>R</i>)-3,5-dihydroxy-7-(4-hydroxyphenyl) heptyl]-1,2-benzenediol (6)	25.86 ± 1.41	35.85 ± 1.55	2833.20 ± 152.74
pinoselinol (7)	235.66 ± 2.37	118.67 ± 2.07	1613.25 ± 61.10
kaempferol (8)	56.92 ± 1.76	18.59 ± 1.27	3526.49 ± 64.29
4- <i>O</i> -methylstroside B (9)	NI	NI	<100
citrulin C (10)	NI	NI	<100
tachioside (11)	NI	118.25 ± 2.07	548.31 ± 33.29
3,4-dimethoxycinnamaldehyde (12)	NI	NI	<100
3-methoxy-4-hydroxycinnamaldehyde (13)	NI	178.17 ± 2.25	539.98 ± 30.00
eugenol (14)	244.25 ± 2.39	135.26 ± 1.55	1084.95 ± 56.79
4-hydroxybenzalacetone (15)	NI	126.85 ± 1.43	426.63 ± 11.52
ascorbic acid ^d	29.81 ± 1.47	31.00 ± 1.49	3351.32 ± 49.35

^aValues represent means ± SD ($n = 3$). ^bDPPH and ABTS⁺: concentration in μM required to scavenge 50% of the radical. ^cFRAP: concentration in μM Trolox equivalents/g. ^dPositive control. ^eNI: $\text{SC}_{50} \geq 500 \mu\text{M}$.

addition, compared with ascorbic acid, compounds **1** ($SC_{50} = 29.96 \pm 1.26 \mu\text{M}$), **2** ($SC_{50} = 29.88 \pm 1.26 \mu\text{M}$), and **5** ($SC_{50} = 30.65 \pm 1.49 \mu\text{M}$) displayed potent antioxidant capacity, while compound **8** ($SC_{50} = 56.92 \pm 1.76 \mu\text{M}$) presented slightly weaker antioxidant capacity than ascorbic acid (Table 3). In the ABTS⁺ assay, compound **8** ($SC_{50} = 18.59 \pm 1.27 \mu\text{M}$) exhibited significant antioxidant activity compared with ascorbic acid ($SC_{50} = 31.00 \pm 1.49 \mu\text{M}$), and compounds **1–4** and **6** displayed potent antioxidant capacity, with SC_{50} values close to that of ascorbic acid. Meanwhile, in FRAP assay, compound **8** ($3526.49 \pm 64.29 \mu\text{mol Trolox/g DW}$) showed the highest ferric reducing power ability at $25 \mu\text{M}$ concentration, compared with ascorbic acid ($3351.32 \pm 49.35 \mu\text{mol Trolox/g DW}$), and compounds **1**, **2**, and **4–6** exhibited a good ferric reducing power ability at the same concentration. The results suggested that the diarylheptanoids had stronger DPPH radical scavenging activity than the other phenolic compounds (with an activity order of **1–6** > **7–15**), while mono-diarylheptanoids displayed higher scavenging activity than bis-diarylheptanoids. In ABTS⁺ assay, compound **8** presented the best antioxidant capacity and compound **6** showed higher antioxidant capacity than compound **5**, which may be due to more hydroxy groups in **6**. Furthermore, in FRAP assay, the phenolic compounds with more phenolic hydroxy groups exhibited a higher ferric reducing power ability.

Inhibitory Effect on Intracellular ROS Generation in H₂O₂-Induced HepG-2 Cells. ROS, which can activate cellular damage when they are excessively produced, are the major etiological factor of oxidative stress and can activate apoptosis.³ H₂O₂ initiates abnormal accumulation of intracellular ROS and induces apoptosis, which is generally used to generate intracellular ROS in *in vitro* models.²⁵ Based on the above results, compounds **1–8** exhibited considerable radical scavenging capacity and were chosen to evaluate intracellular ROS generation in H₂O₂-induced HepG-2 cells. The cytotoxicity of compounds **1–8** was performed on HepG-2 cells using MTT assay (at 2.5, 5, 10, 20, and 40 μM concentrations), which implied that compound **7** had toxicity at 20 μM and all tested samples had no inhibitory effect on HepG-2 cells at 10 μM . Thus, 10 μM of each compound was selected as the test concentration for evaluating the inhibitory effect of intracellular ROS production. After incubating the HepG-2 cells for 24 h, the levels of intracellular ROS of each compound were measured, as shown in Figure 5. The ROS generation ratio was significantly increased to $60.8 \pm 1.95\%$ in the H₂O₂-treated group (model group), compared with the blank control ($24.3 \pm 1.19\%$). Compared with the model group, compounds **1–8** displayed an inhibitory effect on the generation of intracellular ROS with varying degrees ($p < 0.05$). Additionally, compound **3** displayed the strongest inhibitory effect on intracellular ROS production ($p < 0.05$), with the ROS generation ratio close to that of ascorbic acid, followed by compound **5**. Furthermore, compound **3** showed higher inhibitory effect on intracellular ROS production than compound **4**, which may be attributed to hydroxyl groups at C-3 and C-7 or the replacement of glycoside group.

Cytoprotective Activity against H₂O₂-Induced HepG-2 Cell Apoptosis. Apoptosis is a defining process of cell death that is adjusted to proliferation, growth, and mutation of cells. Nevertheless, abnormal apoptosis may lead to untoward effects on the organism.¹ In this study, abnormal apoptosis was induced by 1.0 mM H₂O₂ in HepG-2 cells, and the cell apoptosis percentage was dramatically increased to $30.61 \pm$

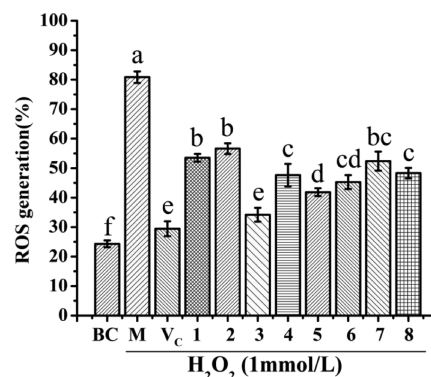


Figure 5. Inhibitory effect of intracellular ROS in H₂O₂-induced HepG-2 cells of the compounds (**1–8**) from *R. beesianus*. All the values are presented as mean \pm SD ($n = 3$). Mean (bar values) with different letters are significantly different ($p < 0.05$). BC: blank control; M: model group (H₂O₂); V_c: positive control (V_c).

1.94%, compared to that of blank control ($5.51 \pm 0.69\%$) ($p < 0.05$). Furthermore, comparing the H₂O₂-treated group (model group, $p < 0.05$), the apoptosis ratios were significantly reduced with different compound-treated groups. All the test compounds (**1–8**, with a concentration at 10 μM) had a significant cytoprotective effect on the H₂O₂-induced HepG-2 cell apoptosis, compared with the model group. Compound **3** showed the strongest efficiency on protecting HepG-2 cells from H₂O₂ toxicity, and the cell apoptosis ratio of **3** ($5.96 \pm 0.36\%$) was close to that of the V_c group (positive control, $9.76 \pm 0.51\%$) and slightly higher than that of the blank control (Figure 6). In addition, compounds **5** and **6** also had considerably better cytoprotective effect, and their cell apoptosis ratios were slightly lower than that of the V_c group. Meanwhile, compounds **4**, **7**, and **8** displayed a moderate cytoprotective effect, and their cell apoptosis ratios are shown in Figure 6. Moreover, different compounds have different protective effects against the H₂O₂-induced apoptosis of HepG-2 cells. The differences of antioxidant capacity may be attributed to the number of phenolic hydroxyl groups and their attachment positions.

CONCLUSIONS

The DPPH, ABTS⁺ radical scavenging, and FRAP assay study results indicated that compounds **1–6** and **8** from *R. beesianus* rhizomes displayed significant antioxidant activities, while compounds **9–13** and **15** were inactive under the same concentration. Hence, structure–antioxidant activity relationships of the diarylheptanoids (**1–6**) were discussed with varying degrees of radical scavenging effects. Compounds **3**, **4**, and **6** presented significant antioxidant activities on DPPH radical scavenging, which suggested that the phenolic hydroxyl groups and the glycoside moiety may play a vital role in scavenging the radicals. Furthermore, compounds **3**, **4**, and **6** exhibited a slightly lower SC_{50} value than compounds **1–2**, which suggested that mono-diarylheptanoids had better antioxidant activities than bis-diarylheptanoids. In the ABTS⁺ and FRAP assays, the diarylheptanoids (**1–6**) except **5** and **8** dramatically scavenged the radicals, while simple phenolic compounds (**7** and **9–15**) did not, which suggested that diarylheptanoids and flavonols probably exhibited better antioxidant activities than simple phenolic compounds.

In summary, 15 phenolic compounds (**1–15**) including three new diarylheptanoids rhynchanines A–C (**1–3**) and one

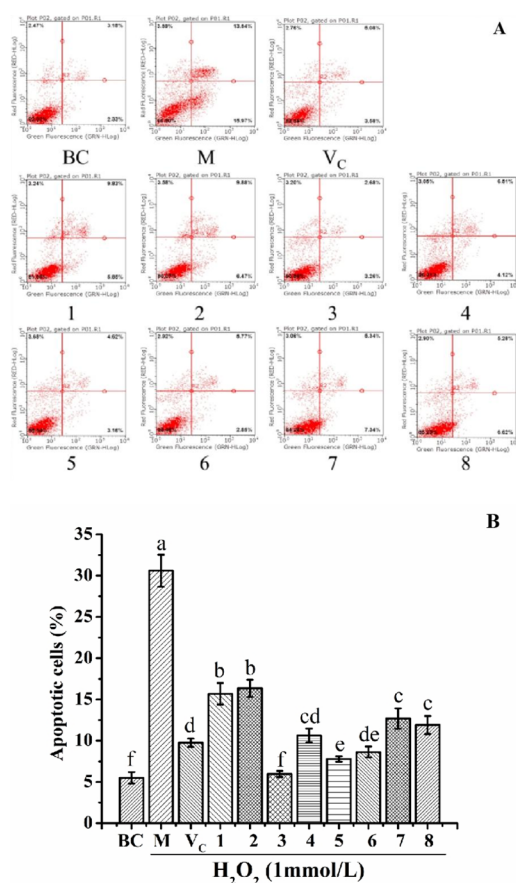


Figure 6. Cytoprotective effect of the compounds (1–8) of *R. beesianus* on apoptosis in H_2O_2 -induced HepG-2 cells. (A) Flow cytometry analysis; (B) apoptotic cell percentage of different groups. All the values are presented as mean \pm SD ($n = 3$). Mean (bar values) with different letters are significantly different ($p < 0.05$). BC: blank control; M: model group (H_2O_2); VC: positive control (V_C).

new phenylpropanoid, 4-*O*-methylstroside B (9), were isolated from *R. beesianus* rhizomes. Most of the isolated compounds displayed significant antioxidant activity on DPPH, ABTS⁺ radical scavenging, and FRAP assays. Furthermore, compounds 3, 5, and 6 could prevent oxidative stress damage through a decrease in ROS content and cell apoptosis in H_2O_2 -induced HepG-2 cells. The antioxidant capacity of different compounds had different effects on DPPH, ABTS⁺ radical scavenging, and FRAP assays. Compound 8 showed the best antioxidant activity in ABTS⁺ and FRAP assays, while it presented moderate antioxidant capacity in DPPH assay. Furthermore, compound 8 moderately inhibited the intracellular ROS production and prevented the cell apoptosis. The results may be attributed to different assays for antioxidant activity. But in most cases, the results of different assays were consistent. Compounds 3, 5, and 6 not only displayed significant antioxidant activity but also prevented oxidative stress damage by inhibiting the intracellular ROS production and cell apoptosis in H_2O_2 -induced HepG-2 cells. Meanwhile, compound 3 possessed more hydroxyl groups and a glycoside moiety, which might be the main promotional factors for antioxidant ability. The diarylheptanoids, especially mono-diarylheptanoids, had stronger antioxidant capacity than the other phenolic compounds (compounds 1–6 > 7–15). Therefore, *R. beesianus* rhizomes might be regarded as a

functional food (antioxidant nutraceuticals) containing antioxidants besides being a kitchen spice.

■ ASSOCIATED CONTENT

Supporting Information

The Supporting Information is available free of charge at <https://pubs.acs.org/doi/10.1021/acs.jafc.1c00869>.

1D and 2D NMR spectra; HRESIMS, UV, and IR spectra of compounds 1–3 and 9; 1D NMR spectra of 3a, 9a, 9aR, 9aS, 4–8, and 10–15; and HPLC profiles of compounds 1–15 (PDF)

■ AUTHOR INFORMATION

Corresponding Authors

Ya-Ping Liu – State Key Laboratory of Phytochemistry and Plant Resources in West China, Kunming Institute of Botany, Chinese Academy of Sciences, Kunming 650201, China; Faculty of Agriculture and Food, Kunming University of Science and Technology, Kunming 650500, China; orcid.org/0000-0002-2164-2489; Phone: +86-0871 65223188; Email: liuyaping@kust.edu.cn

Xiao-Dong Luo – State Key Laboratory of Phytochemistry and Plant Resources in West China, Kunming Institute of Botany, Chinese Academy of Sciences, Kunming 650201, China; Key Laboratory of Medicinal Chemistry for Natural Resource, Ministry of Education and Yunnan Province, School of Chemical Science and Technology, Yunnan University, Kunming 650091, China; orcid.org/0000-0002-6768-5679; Phone: +86-0871 65223177; Email: xdluo@mail.kib.ac.cn

Authors

Pei-Feng Zhu – State Key Laboratory of Phytochemistry and Plant Resources in West China, Kunming Institute of Botany, Chinese Academy of Sciences, Kunming 650201, China; University of Chinese Academy of Sciences, Beijing 100049, China

Gui-Guang Cheng – Faculty of Agriculture and Food, Kunming University of Science and Technology, Kunming 650500, China

Lan-Qin Zhao – State Key Laboratory of Phytochemistry and Plant Resources in West China, Kunming Institute of Botany, Chinese Academy of Sciences, Kunming 650201, China; University of Chinese Academy of Sciences, Beijing 100049, China

Afsar Khan – Department of Chemistry, COMSATS University Islamabad, Abbottabad 22060, Pakistan

Xing-Wei Yang – State Key Laboratory of Phytochemistry and Plant Resources in West China, Kunming Institute of Botany, Chinese Academy of Sciences, Kunming 650201, China; orcid.org/0000-0002-9578-2986

Bu-Yun Zhang – State Key Laboratory of Phytochemistry and Plant Resources in West China, Kunming Institute of Botany, Chinese Academy of Sciences, Kunming 650201, China; University of Chinese Academy of Sciences, Beijing 100049, China

Meng-Cheng Li – Faculty of Agriculture and Food, Kunming University of Science and Technology, Kunming 650500, China

Complete contact information is available at: <https://pubs.acs.org/doi/10.1021/acs.jafc.1c00869>

Author Contributions

#P.-F.Z. and G.-G.C. contributed equally to this work.

Funding

The authors are grateful to Yunnan Major Science and Technology Project in China (2019ZF010, 2019ZF003, and 2019FY003004) for the financial support.

Notes

The authors declare no competing financial interest.

REFERENCES

- (1) Yao, J.; Ge, C.; Duan, D.; Zhang, B.; Cui, X.; Peng, S.; Liu, Y.; Fang, J. Activation of the phase II enzymes for neuroprotection by ginger active constituent 6-Dehydrogingerone in PC12 cells. *J. Agric. Food Chem.* **2014**, *62*, 5507–5518.
- (2) Hao, L.; Gao, X.; Zhou, T.; Cao, J.; Sun, Y.; Dang, Y.; Pan, D. Angiotensin I-converting enzyme (ACE) inhibitory and antioxidant activity of umami peptides after in vitro gastrointestinal digestion. *J. Agric. Food Chem.* **2020**, *68*, 8232–8241.
- (3) Peng, S.; Hou, Y.; Yao, J.; Fang, J. Activation of Nrf2-driven antioxidant enzymes by cardamom confers neuroprotection of PC12 cells against oxidative damage. *Food Funct.* **2017**, *8*, 997–1007.
- (4) Meng, J.; Wang, S.; Liu, Y. Cytoprotection activity evaluation of (E)-3-(3,4-dichloro-phenyl)-1-(3,4-dihydroxyphenyl)-prop-2-en-1-one as a new antioxidant against H₂O₂-induced oxidative damage in PC12 cells. *Pharm. Chem. J.* **2020**, *53*, 942–946.
- (5) Shokoohinia, Y.; Rashidi, M.; Hosseinzadeh, L.; Jelodarian, Z. Quercetin-3-O-β-D-glucopyranoside, a dietary flavonoid, protects PC12 cells from H₂O₂-induced cytotoxicity through inhibition of reactive oxygen species. *Food Chem.* **2015**, *167*, 162–167.
- (6) Blanco Canalis, M. S.; Baroni, M. V.; León, A. E.; Ribotta, P. D. Effect of peach puree incorporation on cookie quality and on simulated digestion of polyphenols and antioxidant properties. *Food Chem.* **2020**, *333*, 127464.
- (7) Zhang, X.; Zhang, M.; Dong, L.; Jia, X.; Liu, L.; Ma, Y.; Huang, F.; Zhang, R. Phytochemical profile, bioactivity, and prebiotic potential of bound phenolics released from rice bran dietary fiber during in vitro gastrointestinal digestion and colonic fermentation. *J. Agric. Food Chem.* **2019**, *67*, 12796–12805.
- (8) Zhu, P.-F.; Zhao, Y.-L.; Dai, Z.; Qin, X.-J.; Yuan, H.-L.; Jin, Q.; Wang, Y.-F.; Liu, Y.-P.; Luo, X.-D. Phenolic amides with immunomodulatory activity from the nonpolysaccharide fraction of *Lycium barbarum* fruits. *J. Agric. Food Chem.* **2020**, *68*, 3079–3087.
- (9) Khalil, A.; Tazeddinova, D. The upshot of Polyphenolic compounds on immunity amid COVID-19 pandemic and other emerging communicable diseases: An appraisal. *Nat. Prod. Bioprospect.* **2020**, *10*, 411–429.
- (10) Lin, Y.; Peng, X.; Ruan, H. Diarylheptanoids from the fresh pericarps of *Juglans hopeiensis*. *Fitoterapia* **2019**, *136*, 104165.
- (11) Jahng, Y.; Park, J.-G. Recent studies on cyclic 1,7-diarylheptanoids: their isolation, structures, biological activities, and chemical synthesis. *Molecules* **2018**, *23*, 3107.
- (12) Bian, Q.-Y.; Wang, S.-Y.; Xu, L.-J.; Chan, C.-O.; Mok, D. K. W.; Chen, S.-B. Two new antioxidant diarylheptanoids from the fruits of *Alpinia oxyphylla*. *J. Asian Nat. Prod. Res.* **2013**, *15*, 1094–1099.
- (13) Manimaran, S.; SambathKumar, K.; Gayathri, R.; Raja, K.; Rajkamal, N.; Venkatchalapathy, M.; Ravichandran, G.; Lourdu EdisonRaj, C. Medicinal plant using ground state stabilization of natural antioxidant curcumin by Keto-Enol tautomerisation. *Nat. Prod. Bioprospect.* **2018**, *8*, 369–390.
- (14) Wu, H.-C.; Cheng, M.-J.; Peng, C.-F.; Yang, S.-C.; Chang, H.-S.; Lin, C.-H.; Wang, C.-J.; Chen, I.-S. Secondary metabolites from the stems of *Engelhardia roxburghiana* and their antitubercular activities. *Phytochemistry* **2012**, *82*, 118–127.
- (15) Thongon, N.; Boonmuen, N.; Suksen, K.; Wichit, P.; Chairoungdua, A.; Tuchinda, P.; Suksamram, A.; Winuthayanon, W.; Piyachaturawat, P. Selective estrogen receptor modulator (serm)-like activities of diarylheptanoid, a phytoestrogen from *Curcuma comosa*, in breast cancer cells, pre-osteoblast cells, and rat uterine tissues. *J. Agric. Food Chem.* **2017**, *65*, 3490–3496.
- (16) Haniadka, R.; Saldanha, E.; Sunita, V.; Palatty, P. L.; Fayad, R.; Baliga, M. S. A review of the gastroprotective effects of ginger (*Zingiber officinale* Roscoe). *Food Funct.* **2013**, *4*, 845–855.
- (17) Wohlmuth, H.; Deseo, M. A.; Brushett, D. J.; Thompson, D. R.; MacFarlane, G.; Stevenson, L. M.; Leach, D. N. Diarylheptanoid from *Pleuranthodium racemigerum* with in Vitro prostaglandin E2 inhibitory and cytotoxic activity. *J. Nat. Prod.* **2010**, *73*, 743–746.
- (18) Gao, J.-Y.; Yang, Z.-H.; Ren, P.-Y.; Li, Q.-J. Reproductive ecology of *Rhynchanthus beesianus* W. W Smith (Zingiberaceae) in south yunnan, China: a ginger with bird pollination syndrome. *J. Integr. Plant Biol.* **2006**, *48*, 1294–1299.
- (19) Zhou, L. Chemical constituents of *Rhynchanthus beesianus* oil. *Flavour Fragrance Cosmetics* **2006**, *2*, 15–16.
- (20) Wei, A.; Hou, H.-B.; Xia, T.-L.; Yang, L.-R. Study on antibacterial activity and stability of edible *Rhynchanthus beesianus* essential oil in vitro. *China Food Addit.* **2019**, 49–54.
- (21) Zhao, X.-G.; Chen, Q.; Lu, T.-Y.; Wei, F.; Yang, Y.; Xie, D.; Wang, H.-J.; Tian, M.-Y. Chemical composition, antibacterial, anti-inflammatory, and enzyme inhibitory activities of essential oil from *Rhynchanthus beesianus* rhizome. *Molecules* **2021**, *26*, 167.
- (22) Jin, S.; Song, C.; Jia, S.; Li, S.; Zhang, Y.; Chen, C.; Feng, Y.; Xu, Y.; Xiong, C.; Xiang, Y.; Jiang, H. An integrated strategy for establishment of curcuminoid profile in turmeric using two LC-MS/MS platforms. *J. Pharm. Biomed. Anal.* **2017**, *132*, 93–102.
- (23) Wang, X.; Gao, A.; Jiao, Y.; Zhao, Y.; Yang, X. Antitumor effect and molecular mechanism of antioxidant polysaccharides from *Salvia miltiorrhiza* Bunge in human colorectal carcinoma LoVo cells. *Int. J. Biol. Macromol.* **2018**, *108*, 625–634.
- (24) Bruhn, T.; Schaumlöffel, A.; Hemberger, Y.; Bringmann, G. SpecDis: quantifying the comparison of calculated and experimental electronic circular dichroism spectra. *Chirality* **2013**, *25*, 243–249.
- (25) Li, T.-X.; Meng, D.-D.; Guo, Y.-X.; Bai, B.; Xu, G.-G.; Yang, Y.-N.; Xie, X.-Y.; Wang, Y.; Xu, C.-P. Antioxidant epoxydon and benzolactone derivatives from the insect-associated fungus *Phoma* sp. *J. Asian Nat. Prod. Res.* **2020**, *22*, 647–654.
- (26) Ma, R.-J.; Yang, L.; Bai, X.; Li, J.-Y.; Yuan, M.-Y.; Wang, Y.-Q.; Xie, Y.; Hu, J.-M.; Zhou, J. Phenolic Constituents with antioxidative, tyrosinase inhibitory and anti-aging activities from *Dendrobium loddigesii* Rolfe. *Nat. Prod. Bioprospect.* **2019**, *9*, 329–336.
- (27) Yang, M.; Ma, Y.; Wang, Z.; Khan, A.; Zhou, W.; Zhao, T.; Cao, J.; Cheng, G.; Cai, S. Phenolic constituents, antioxidant and cytoprotective activities of crude extract and fractions from cultivated *Artichoke inflorescence*. *Ind. Crops Prod.* **2020**, *143*, 111433.
- (28) Sun, D.; Huang, S.; Cai, S.; Cao, J.; Han, P. Digestion property and synergistic effect on biological activity of purple rice (*Oryza sativa* L.) anthocyanins subjected to a simulated gastrointestinal digestion in vitro. *Food Res. Int.* **2015**, *78*, 114–123.
- (29) Ali, M. S.; Tezuka, Y.; Banskota, A. H.; Kadota, S. Blepharocalyxins C-E, three new dimeric diarylheptanoids, and related compounds from the seeds of *Alpinia blepharocalyx*. *J. Nat. Prod.* **2001**, *64*, 491–496.
- (30) Liu, D.; Liu, Y.-W.; Guan, F.-Q.; Liang, J.-Y. New cytotoxic diarylheptanoids from the rhizomes of *Alpinia officinarum* Hance. *Fitoterapia* **2014**, *96*, 76–80.
- (31) Lin, Y.-S.; Lin, J.-H.; Chang, C.-C.; Lee, S.-S. Tetrahydropyran- and Tetrahydrofuran- containing diarylheptanoids from *Hedychium coronarium* rhizomes. *J. Nat. Prod.* **2015**, *78*, 181–187.
- (32) Maehara, S.; Ikeda, M.; Haraguchi, H.; Kitamura, C.; Nagoe, T.; Ohashi, K.; Shibuya, H. Microbial conversion of curcumin into colorless hydroderivatives by the endophytic fungus *Diaporthe* sp. associated with *Curcuma longa*. *Chem. Pharm. Bull.* **2011**, *59*, 1042–1044.
- (33) Dong, S.-H.; Nikolić, D.; Simmler, C.; Qiu, F.; van Breemen, R. B.; Soejarto, D. D.; Pauli, G. F.; Chen, S.-N. Diarylheptanoids from *Dioscorea villosa* (Wild Yam). *J. Nat. Prod.* **2012**, *75*, 2168–2177.

- (34) Fu, G.; Zhang, W.; Du, D.; Ng, Y. P.; Ip, F. C. F.; Tong, R.; Ip, N. Y. Diarylheptanoids from rhizomes of *Alpinia officinarum* inhibit aggregation of α -synuclein. *J. Agric. Food Chem.* **2017**, *65*, 6608–6614.
- (35) He, X.-F.; Zhang, X.-K.; Geng, C.-A.; Hu, J.; Zhang, X.-M.; Guo, Y.-Q.; Chen, J.-J. Tsaokopyranols A-M, 2,6-epoxydiarylheptanoids from *Amomum tsao-ko* and their α -glucosidase inhibitory activity. *Bioorg. Chem.* **2020**, *96*, 103638.
- (36) Li, W.; Wang, S.; Feng, J.; Xiao, Y.; Xue, X.; Zhang, H.; Wang, Y.; Liang, X. Structure elucidation and NMR assignments for curcuminoids from the rhizomes of *Curcuma longa*. *Magn. Reson. Chem.* **2009**, *47*, 902–908.
- (37) Kikuzaki, H.; Hara, S.; Kawai, Y.; Nakatani, N. Antioxidative phenylpropanoids from berries of *Pimenta dioica*. *Phytochemistry* **1999**, *52*, 1307–1312.
- (38) Yokosuka, A.; Mimaki, Y.; Sakagami, H.; Sashida, Y. New diarylheptanoids and diarylheptanoid glucosides from the rhizomes of *Tacca chantrieri* and their cytotoxic activity. *J. Nat. Prod.* **2002**, *65*, 283–289.
- (39) Carpinella, M. C.; Giorda, L. M.; Ferrayoli, C. G.; Palacios, S. M. Antifungal effects of different organic extracts from *Melia azedarach* L. on Phytopathogenic fungi and their isolated active components. *J. Agric. Food Chem.* **2003**, *51*, 2506–2511.
- (40) Mei, W.-L.; Chen, C.-X.; Wu, G.-F. Flavonoids from *Cinnamomum zeylanicum*. *Acta Botanica Yunnanica* **2001**, *23*, 394–396.
- (41) Teng, R. W.; Wang, D. Z.; Wu, Y. S.; Lu, Y.; Zheng, Q. T.; Yang, C. R. NMR assignments and single-crystal X-ray diffraction analysis of deoxyloganic acid. *Magn. Reson. Chem.* **2005**, *43*, 92–96.
- (42) Pedras, M. S. C.; Zheng, Q.-A. Metabolic responses of *Theilungiella halophila/salsuginea* to biotic and abiotic stresses: Metabolite profiles and quantitative analyses. *Phytochemistry* **2010**, *71*, 581–589.
- (43) Jolad, S. D.; Lantz, R. C.; Chen, G. J.; Bates, R. B.; Timmermann, B. N. Commercially processed dry ginger (*Zingiber officinale*): Composition and effects on LPS-stimulated PGE2 production. *Phytochemistry* **2005**, *66*, 1614–1635.
- (44) Elgendy, E. M.; Khayyat, S. A. Oxidation reactions of some natural volatile aromatic compounds: anethole and eugenol. *Russ. J. Org. Chem.* **2008**, *44*, 823–829.
- (45) Chakraborti, A. K.; Sharma, L.; Nayak, M. K. Demand-based thiolate anion generation under virtually neutral conditions: influence of steric and electronic factors on chemo- and regioselective cleavage of aryl alkyl ethers. *J. Org. Chem.* **2002**, *67*, 6406–6414.